Assessment of extracellular matrix-related biomarkers in patients with lower extremity artery disease

Anna Hernández-Aguilera, PhD,[a] Signe Holm Nielsen, MS,[b,c] Cristina Bonache, BS,[a] Salvador Fernández-Arroyo, PhD,[a] Vicente Martín-Paredero, PhD, MD,[d] Montserrat Fibla, PhD,[a,e] Morten A. Karsdal, PhD,[b] Federica Genovese, PhD,[b] Javier A. Menendez, PhD,[f] Jordi Camps, PhD,[a] *and* Jorge Joven, PhD, MD,[a] *Reus, Tarragona, and Girona, Spain; and Herlev and Kongens Lyngby, Denmark*

ABSTRACT

Background: The prevalence of lower extremity artery disease (LEAD) is high (20%-25%) in the population older than 65 years, but patients are seldom identified until the disease is advanced. Circulating markers of disease activity might provide patients with a key opportunity for timely treatment. We tested the hypothesis that measuring blood-specific fragments generated during degradation of the extracellular matrix (ECM) could provide further insight into the pathophysiologic mechanism of arterial remodeling.

Methods: The protein profile of diseased arteries from patients undergoing infrainguinal limb revascularization was assessed by a liquid chromatography and tandem mass spectrometry, nontargeted proteomic approach. The information retrieved was the basis for measurement of neoepitope fragments of ECM proteins in the blood of 195 consecutive patients with LEAD by specific enzyme-linked immunosorbent assays.

Results: Histologic and proteomic analyses confirmed the structural disorganization of affected arteries. Fourteen of 81 proteins were identified as differentially expressed in diseased arteries with respect to healthy tissues. Most of them were related to ECM components, and the difference in expression was used in multivariate analyses to establish that severe arterial lesions in LEAD patients have a specific proteome. Analysis of neoepitope fragments in blood revealed that fragments of versican and collagen type IV, alone or in combination, segregated patients with mild to moderate symptoms (intermittent claudication, Fontaine I-II) from those with severe LEAD (critical limb ischemia, Fontaine III-IV).

Conclusions: We propose noninvasive candidate biomarkers with the ability to be clinically useful across the LEAD spectrum. (J Vasc Surg 2018;68:1135-42.)

Keywords: Atherosclerosis; Biomarker; Collagen; Extracellular matrix; Neoepitopes; Peripheral artery disease; Versican

Atherosclerosis is a progressive, age-related disease that may simultaneously affect multiple arteries. The interest in noncoronary atherosclerosis is increasing because patients with manifestations in several vascular beds have poorer prognosis than those with just one territory affected.[1] This association is particularly evident in patients with lower extremity artery disease (LEAD; also known as peripheral artery disease, PAD). There are >200 million patients with LEAD in industrialized countries, and the convergent epidemics of diabetes and obesity suggest bleak prospects.[1,2] Despite its major prognostic impact, limited information is available on asymptomatic PAD. The life expectancy of a patient with either intermittent claudication (IC) or critical limb ischemia (CLI) is low, and once diagnosed, patients have significantly less chance of receiving risk factor modification than patients with coronary disease.[3,4] The challenge is to establish whether lesions in lower extremity arterial occlusive disease have a specific proteome and to propose noninvasive surrogates to anticipate prevention strategies.

Locoregional hemodynamic and rheologic factors favor the progression of atherosclerotic lesions in lower extremity arteries, and reduction in lumen caliber governs the course of symptoms in patients with LEAD.[5] Vessel wall remodeling and angiogenesis in peripheral arteries appear to be crucial processes to understanding of the overall response to atherosclerotic injuries.[6] In this scenario, the

From the Unitat de Recerca Biomèdica, Hospital Universitari Sant Joan, Institut d'Investigació Sanitària Pere Virgili, Universitat Rovira i Virgili, Reus[a]; the Fibrosis Biology and Biomarkers, Nordic Bioscience, Herlev[b]; the Department of Biotechnology and Biomedicine, Technical University of Denmark, Kongens Lyngby[c]; the Department of Vascular Surgery,[d] and Department of Pathology,[e] Hospital Universitari Joan XXIII, Tarragona; and the Molecular Oncology Group, Girona Biomedical Research Institute (IDIBGI), Girona.[f]

Current work in Prof Joven's laboratories is supported by grants from the Plan Nacional de I+D+I, Spain; Instituto de Salud Carlos III (PI15/00285, cofounded by the European Regional Development Fund); Agència de Gestió d'Ajuts Universitaris i de Recerca (2014 SGR1227); and Fundació La Marató de TV3. The Danish Research Foundation also supported this work. The decision to submit the manuscript for publication is the sole responsibility of the investigators.

Author conflict of interest: S.H.N., M.A.K., and F.G. are full-time employees of Nordic Bioscience, and M.A.K. holds stock in Nordic Bioscience.

Additional material for this article may be found online at www.jvascsurg.org.

Correspondence: Jorge Joven, PhD, MD, Unitat de Recerca Biomèdica, Hospital Universitari Sant Joan, Institut d'Investigació Sanitària Pere Virgili, Universitat Rovira i Virgili, Carrer Sant Llorenç 21, 43201 Reus, Spain (e-mail: jorge.joven@urv.cat).

The editors and reviewers of this article have no relevant financial relationships to disclose per the JVS policy that requires reviewers to decline review of any manuscript for which they may have a conflict of interest.

0741-5214

https://doi.org/10.1016/j.jvs.2017.12.071

extracellular matrix (ECM) provides a mechanical scaffold and support to cell migration, which is regulated by the correct functioning of cytokines, enzymes such as matrix metalloproteinases (MMPs), and growth factors.[7-9] Atherosclerosis-associated remodeling and disrupted cytoskeletal architecture are the consequence of inflammatory cell activity, lipid deposition, and changes in ECM balance.[10-14] We address the proteome composition and the relative expression of ECM components in severely affected peripheral arteries to evaluate different neoepitope biomarkers of ECM degradation measured in serum from PAD patients to assess whether these markers might be associated with disease activity.

ARTICLE HIGHLIGHTS

- **Type of Research:** Histologic and proteomic analyses of human arteries removed during surgical revascularization
- **Take Home Message:** Compared with healthy controls, multiple extracellular matrix proteins were identified and validated by enzyme-linked immunosorbent assay to confirm identity and expression levels. In particular, fragments of versican and collagen type IV allowed discrimination of peripheral artery disease severity.
- **Recommendation:** Data suggest that multiple extracellular matrix serum profile screening in peripheral artery disease patients may have utility in discriminating mild to severe disease.

METHODS

Participants and study design. The local Ethics Committee and Institutional Review Board approved the procedures involved in this study (Epinols/12-03-09/3proj6; Inflamet/15-04-30/4proj6). First, histologic and proteomic analyses were performed in portions of superficial femoral arteries that included the entire artery wall from patients requiring infrainguinal limb revascularization ($n = 18$) and controls ($n = 3$) obtained from road accident victims of similar age. Written informed consent was obtained from participants or next of kin. Demographic and cardiovascular risk profiles of control individuals and PAD patients used for these analyses can be found in the Supplementary Methods and Supplementary Table I (online only). To limit likely sex differences and because the disease is more prevalent in men, we then recruited men with an established diagnosis of PAD attending our Department of Vascular Surgery. There were 195 participants included. Serum was collected at the time of inclusion, identified according to Fontaine classification,[15] and stored at −80°C until analyses. Exclusion criteria were clinically assessed; patients with infected lesions, evidence of recent neoplastic disease, chronic kidney disease, liver disease, or inflammatory disease (or receiving anti-inflammatory drugs) were excluded. Ankle-brachial index (ABI) was measured per standard technique in both lower limbs, and imaging techniques were performed according to the standard of care.

Histologic examination. To examine tissue morphologic features, serial sections of tissue were obtained from samples fixed in 10% neutral buffered formalin and embedded in paraffin. Hematoxylin and eosin staining (Sigma-Aldrich, Steinheim, Germany) was used to identify different cellular structures. Masson trichrome staining (Bio Optica, Milan, Italy) was used to assess collagen fibers, smooth muscle cells, nucleus, and cytoplasm, and sirius red staining (direct red 80; Sigma-Aldrich) was used to identify collagen fibers. Images were obtained at 200× magnification, and the intima-media ratio was obtained by dividing the thickness of the intima by the thickness of the media measured using an optical microscope (Eclipse E600; Nikon, Madrid, Spain) equipped with image analysis.

Untargeted proteomics. To explore the proteome composition of the arteries, we used a nondirected proteomic approach. Proteomics experiments were exploratory, with extensive mapping of digested peptides to identify and to quantify as many proteins as possible, and performed using chemical labeling to differentiate groups. Methods were similar to those previously used to analyze the protein secretion profile of carotid atherosclerotic plaques.[16] Specific details may be found in the Supplementary Methods (online only). Briefly, sample arteries were cut into pieces and homogenized in the presence of type 1 collagenase (Sigma-Aldrich). Following different rounds of centrifugation and chemical treatment, precipitated proteins were vacuum dried and dissolved. Samples were then sequentially denatured, reduced, and alkylated. For digestion, samples were incubated with sequencing-grade trypsin overnight at 37°C. We used a liquid chromatography-mass spectrometry (MS) approach for quantification by performing isobaric tag for relative and absolute quantitation (iTRAQ) labeling with iTRAQ 8-plex reagent kits (SCIEX, Madrid, Spain), as previously described.[17] Labeled peptides were then purified using an SCX column (Strata SCX 55 μm, 70Å; Phenomenex, Torrance, Calif), desalted and concentrated through a C18 Sep-Pak column (Waters, Bedford, Mass), and analyzed by using a C18 reversed phase nanocolumn coupled to a trap nanocolumn for real-time ionization and peptide fragmentation on an LTQ Orbitrap Velos Pro mass spectrometer (Thermo Fisher Scientific, San Jose, Calif). To identify proteins, information was obtained from tandem mass spectra with the aid of Proteome Discoverer (version 1.4.0.288; Thermo Fisher Scientific). All MS and tandem MS (MS/MS) samples were analyzed using Mascot (version 2.4.1.0; Thermo Fisher Scientific). Protein

quantification was performed by comparing the peak intensity of the reporter ions in the MS/MS spectra to that of the selected peptides to assess the relative abundance of the peptides. Normalized concentrations (logarithmic) of selected proteins were used to assess the increased or decreased expression of proteins in LEAD arteries.

Enzyme-linked immunosorbent assays. The selected biomarkers were chosen on the basis of the obtained proteomic data, pathway analysis according to the ConsensusPathDB-human platform, and previously published data.[18,19] Measurements were performed at Nordic Bioscience (Herlev, Denmark) laboratories using their developed competitive enzyme-linked immunosorbent assays. Specifications of the assays are available in Supplementary Table II (online only).

Statistical analysis. The Kolmogorov-Smirnov test was used to assess normal distribution of the variables. We used the Mann-Whitney *U* test to compare nonparametric variables, Student *t*-test for parametric variables, and contingency tables and the χ^2 test for categorical variables. For multiple comparisons, the Kruskal-Wallis test or analysis of variance (one-way analysis of variance) was used. The results were expressed as median and interquartile range or percentage of the total participants. For proteomic analyses, principal component analysis and hierarchical clustering analysis were performed using the Mass Profiler Professional software (version 12.1; Agilent Technologies, Santa Clara, Calif). Only proteins that appeared in >70% of the samples were considered, and the PANTHER system (www.pantherdb.org) was used for functional classification. We used the Benjamini-Hochberg method to avoid false positives in differences due to multiple testing. Analyses with receiver operating characteristic curves, linear regression, and binary logistic regression were performed using the Statistical Package for the Social Sciences, version 22.0 (IBM Corp, Armonk, NY). MetaboAnalyst 3.0 (http://www.metaboanalyst.ca/) was used to generate scores/loading plots, heatmaps, and random forest analysis.

RESULTS

We first evaluated, combining histology and untargeted proteomics, the differences in the integrity of arterial tissue and signs of vascular remodeling, in severely lesioned and healthy arteries, to confirm that samples from PAD patients were representative of the pathologic state. Atherosclerosis was evident in all samples from PAD patients (Supplementary Fig, online only). To mitigate run-to-run variability, we quantified samples that have been multiplexed, covalently labeled, and then combined in a single run containing multiple samples. Peptides present in <70% of the samples in both control and PAD arteries and those generating similar fingerprint spectra were not considered in further data-dependent analyses (Supplementary Table III, online only). Under these conditions, this proteomics approach selected 81 proteins, and quantitative analysis revealed a unique subset of 14 proteins with statistically significant differences between diseased and healthy arteries (Fig 1, *A*). Their putative functions in atherosclerosis (Supplementary Table III, online only) disclosed that most of these proteins were ECM or cytoskeletal components (Fig 1, *B*). Hierarchical clustering analyses and principal component analysis strongly suggest that severe disease in PAD patients may have a specific proteome, as illustrated in Fig 1, *C-E*. The identified proteins suggested an imbalance favoring degradation of ECM proteins. Because of histologic changes in collagen and proteomic differences in versican, we selected specific neoepitope fragments of proteins describing the turnover of the major components of vascular ECM: versican, type IV collagen, mimecan, and laminin. Degradation fragments of C-reactive protein and α-smooth muscle actin were also included to investigate the influence of the inflammatory and fibroblastic components, respectively (Supplementary Table II, online only).

The clinical characteristics and laboratory measurements confirmed that the cohort of patients used for these measurements is representative of the clinical spectrum of PAD patients seeking attention in our facilities. The high prevalence of cardiovascular risk factors (such as smoking habits) and other associated treatment (mainly statins) did not significantly affect disease severity, with the exception of a lower prevalence of diabetes in Fontaine I patients. Age was also significantly associated with disease severity (Table I). The concentration of the selected neoepitope biomarkers in serum of PAD patients with different Fontaine stages is indicated in Table II. Initially, specific fragments of MMP-8- and MMP-12-mediated degradation of versican (VCANM), of MMP-9-mediated degradation of α5 chain of laminin (Lam-a5), and of MMP-12-mediated degradation of α1 chain of type IV collagen (C4M) could separate patients in different disease stages. This was further confirmed for VCANM and C4M by using random forest analyses, but Lam-a5 levels failed to discriminate patients with IC from those with CLI. Serum VCANM concentration decreased progressively and was correlated with clinical severity. The analysis of receiver operating characteristic curves displayed a high sensitivity and specificity to distinguish between patients classified as type I from those with type IV (Fig 2, *A* and *B*). A similar discriminative value was obtained for C4M, but circulating levels were increased according to disease severity (Fig 2, *C* and *D*). The combination of both potential biomarkers provided specificity higher than 90% to discriminate between patients with mild IC and those with severe PAD (Fig 2, *E*), and none of them were associated with age or diabetes, the main risk factors for our PAD population. However, the standard technique for PAD diagnosis, the ABI, showed the best discriminant capacity (Fig 2, *F*).

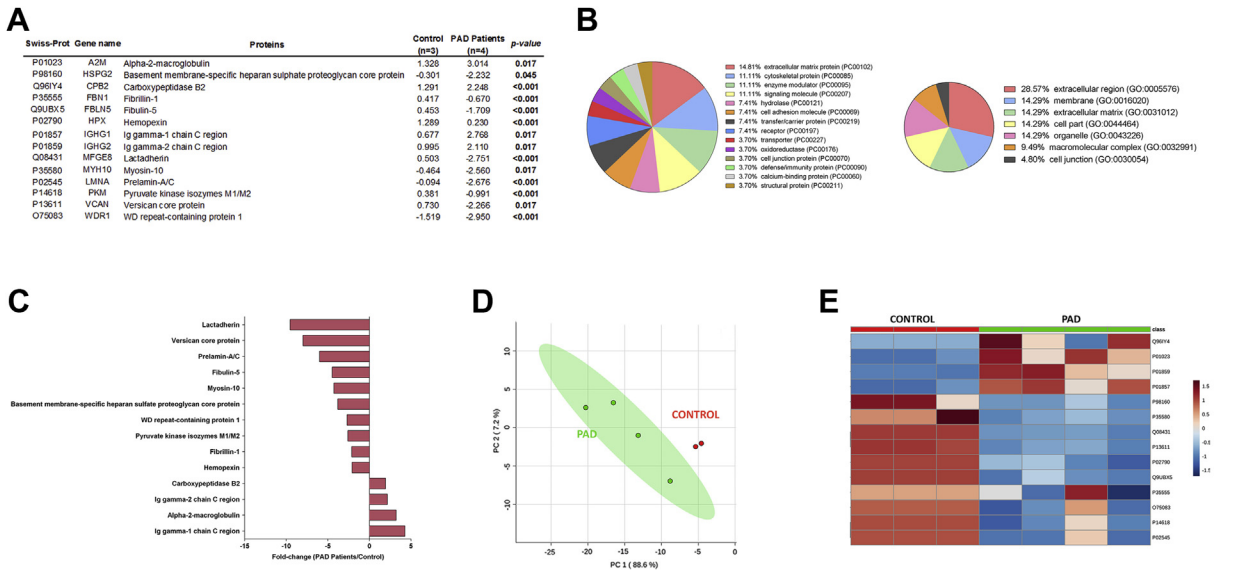

Fig 1. Proteomics analysis: representative results of one 8-plex array. **A,** Proteins showing statistically significant differences between control group and peripheral artery disease (*PAD*) patients. **B,** Protein class (*left*) and cellular component (*right*) percentage of selected proteins obtained by PANTHER system. **C,** Representation of the fold changes obtained using normalized concentrations of selected proteins in both groups. **D** and **E,** Principal component analysis **(D)** and heatmap diagram **(E)** of proteomics results. *Q96IY4*, Carboxypeptidase B2; *P01023*, α_2-macroglobulin; *P01859*, immunoglobulin γ2 chain C region; *P01857*, immunoglobulin γ1 chain C region; *P98160*, basement membrane-specific heparan sulfate proteoglycan core protein; *P35580*, myosin 10; *Q08431*, lactadherin; *P13611*, versican core protein; *P02790*, hemopexin; *Q9UBX5*, fibulin 5; *P35555*, fibrillin 1; *O75083*, WD repeat-containing protein 1; *P14618*, pyruvate kinase isozymes M1/M2; *P02545*, prelamin A/C.

DISCUSSION

The clinical and prognostic relevance of atherosclerosis in the peripheral arteries of the lower limbs deserves further awareness by the medical community, but LEAD remains underdiagnosed and undertreated.[20] The relevance of risk factors, the role of drug prevention, and the causes of differential progression in noncoronary atherosclerosis have been scarcely investigated.[21] Organization models focused on a broad cardiovascular concept are currently an unmet need, which is hampered by the lack of biomarkers able to detect the asymptomatic stages and to predict or to monitor disease progression.

Our findings confirm that atherosclerosis of the lower extremities may be a model to study arterial remodeling. In limb arteries, the lumen loss is not due to neointima formation but to an excessive reparative response, which includes factors favoring ECM degradation.[22] The specific proteome we have described of severe atherosclerotic lesions in peripheral arteries indicates that some proteins are overexpressed. For example, α_2-macroglobulin and carboxypeptidase B2 contribute to the differences observed between diseased and control arteries. α_2-Macroglobulin has recently been associated with plaque vulnerability in carotid arteries using a similar iTRAQ-based analysis,[23] and carboxypeptidase B2 may be a potential indicator of a high risk of premature PAD.[24] Conversely, other proteins were significantly decreased in diseased arteries compared with controls and are mostly related to tissue modeling and remodeling. Among them, low levels of lactadherin may indicate poor adhesion of smooth muscle cells to elastin fibers.[25] Decreased levels of structural proteins, which include versican, laminin, and mimecan, are highly influenced by MMP activity. These proteins also have defined roles in the maintenance of normal cardiovascular function and migration of smooth muscle cells.[26-29] Taken together, our results indicate the coexistence of multiple mechanisms acting simultaneously in response to atherosclerotic injury.

The results also highlight the central role of connective tissue turnover in the structural and signaling properties of arterial cells in LEAD.[14] With the rationale that measuring specific neoepitopes reflecting ECM turnover in the blood of our patients might contribute to the search for biomarkers of disease activity, we tested selected variables for evaluation.[30-33] Among these circulating neoepitopes, those generated from α-smooth muscle actin and laminin α5 showed some potential by correlating with individual clinical end points (Supplementary Table II, online only; Table I), but our focus was on clinically separating patients with mild PAD (IC, Fontaine I-II) from those with severe PAD (CLI, Fontaine III-IV). Serum concentrations of versican (VCANM) and type IV collagen (C4M) degradation products were the most accurate separators. The activities of MMPs in fibroproliferative diseases are well

Table I. Clinical characteristics, complete blood count, and biochemical characteristics of peripheral artery disease (PAD) patients segregated by Fontaine classification

	Fontaine I (n = 11)	Fontaine II (n = 41)	Fontaine III (n = 34)	Fontaine IV (n = 109)	*P* value
Clinical characteristics					
Age, years	55 (50-69)	70 (59.25-75)	63 (55-69.25)	71 (64-77)	<.001
BMI, kg/m^2	28.9 (23.05-31.16)	27.3 (23-29.4)	25.5 (22.25-27.9)	24 (22-27.8)	NS
Diabetes	10	69.4	45.5	79.8	<.001
Hypertension	50	63.2	57.6	75	NS
Dyslipidemia	55.6	41.7	24.2	36.7	NS
Complete blood count					
Red blood cells, $\times10^{12}$/L	5.11 (4.41-5.4)	4.48 (3.95-4.79)	4.29 (3.74-4.53)	4.00 (3.34-4.59)	<.001
Hemoglobin, g/dL	14.6 (13.23-16.35)	13.1 (11.5-15.2)	13.57 (12.02-14.07)	11.5 (10.5-13.5)	.02
Leukocytes, $\times10^9$/L	7.44 (6.85-10.23)	7.51 (6.3-9.42)	7.61 (6.39-9.56)	8.35 (6.4-10.1)	NS
Platelets, $\times10^9$/L	217.25 (186-243.5)	219 (183-268)	252 (200.5-333.65)	270 (209.5-343)	.011
Biochemical variables					
Total cholesterol, mmol/L	4.06 (2.84-5.65)	4.04 (3.72-4.74)	3.95 (3.37-4.47)	3.77 (3.1-4.51)	NS
HDL cholesterol, mmol/L	0.8 (0.72-1.14)	1.1 (0.86-1.29)	1.1 (0.87-1.26)	0.92 (0.74-1.14)	NS
LDL cholesterol, mmol/L	2.04 (1.4-3.32)	2.41 (1.94-3.4)	2.2 (1.73-2.81)	2.18 (1.72-2.83)	NS
Triglycerides, mmol/L	1.56 (1.18-4.53)	1.51 (1.14-2.56)	2.35 (1.87-3.47)	1.97 (1.37-2.86)	NS
Glucose, mmol/L	6.69 (4.1-7.64)	5.93 (4.96-8.82)	5.59 (4.62-7.49)	5.77 (4.59-7.6)	NS
ALT, U/L	19 (12.14-35)	21 (16-26)	22 (16-40)	21 (13-32)	NS
GGT, U/L	27.5 (16.94-39.8)	28 (18-47)	24 (17.25-43)	31.5 (17-48.8)	NS
AST, U/L	21 (12-27)	19 (16-22)	20 (14.75-31)	19 (15-30)	NS
Fibrinogen, g/L	4.07 (3.6-5.48)	4.84 (4.12-6.43)	5.39 (4.27-6.11)	5.82 (4.44-7.78)	NS

ALT, Alanine transaminase; *AST,* aspartate transaminase; *BMI,* body mass index; *GGT,* γ-glutamyltransferase; *HDL,* high-density lipoprotein; *LDL,* low-density lipoprotein; *NS,* not significant.
Nonparametric variables are shown as median (25%-75% interquartile range). Qualitative variables are expressed as percentage of total participants. Statistical differences were assessed by Kruskal-Wallis test.

Table II. Differences in selected neoepitopes between peripheral artery disease (PAD) patients segregated by Fontaine classification

	Fontaine I (n = 11)	Fontaine II (n = 41)	Fontaine III (n = 34)	Fontaine IV (n = 109)	*P* value
VCANM, pg/mL	1800 (1640-1900)	1610 (1375-1830)	1530 (1055-1810)	1250 (1080-1560)	<.001
C4M, pg/mL	16,530 (13,720-21,710)	21,480 (16,860-30,120)	24,790 (18,095-31,940)	31,730 (22,415-45,165)	<.001
Lam-a5, pg/mL	5610 (4630-8490)	6660 (4855-9810)	6130 (3928-8278)	8710 (6755-11,960)	<.001
CRPM, pg/mL	7620 (5690-11,520)	9380 (6780-14,100)	8645 (6615-11,590)	9970 (7775-12,430)	NS
α-SMA, pg/mL	3870 (2830-4900)	3620 (2770-5570)	3355 (2283-4513)	3600 (2430-5100)	NS
MIM, pg/mL	7600 (3600-20,370)	7430 (3770-12,090)	6770 (2795-13,635)	8070 (3885-13,290)	NS

C4M, Matrix metalloproteinase (MMP)-12-mediated type IV (α1) collagen degradation; *CRPM,* specific fragment of MMPs 1-, 3-, 8-, and 9-, CatS/K-, ADAMTS1-mediated degradation of C-reactive protein; *Lam-a5,* specific fragment of MMP-9-mediated laminin α5 chain degradation; *MIM,* specific fragment of MMP-9- and MMP-12-mediated degradation of mimecan; *NS,* not significant; *α-SMA,* α-smooth muscle actin, acetylated N-terminal; *VCANM,* specific fragment of MMP-8- and MMP-12-mediated degradation of versican.
Results are expressed as median (interquartile range) for nonparametric variables. Statistical differences were assessed by Kruskal-Wallis test.

established and probably are partially implicated in these findings.[34,35] Although our study is not performed in a prospective cohort, results suggest that disease progression might be associated with a decrease in VCANM levels and an increase in C4M levels. However, these patients are clinically complex and taking statins or other drugs. Consequently, interpretation should be cautious.

Versican and other proteoglycans, synthesized by vascular smooth muscle cells and influenced by growth factors, play a fundamental role in cellular and extracellular events associated with the pathogenesis of vascular lesions.[36,37] Circulating VCANM neoepitopes were inversely associated with lesion progression, and results were consistent with proteomic analysis and histologic findings indicating advanced fibroatheroma and calcium accumulation. Presumably, the digestion of versican results from increasing infiltration by macrophages, but the complex proteolytic events generating relevant versican fragments have not been explored in vivo. Conversely, circulating C4M levels may serve as a useful

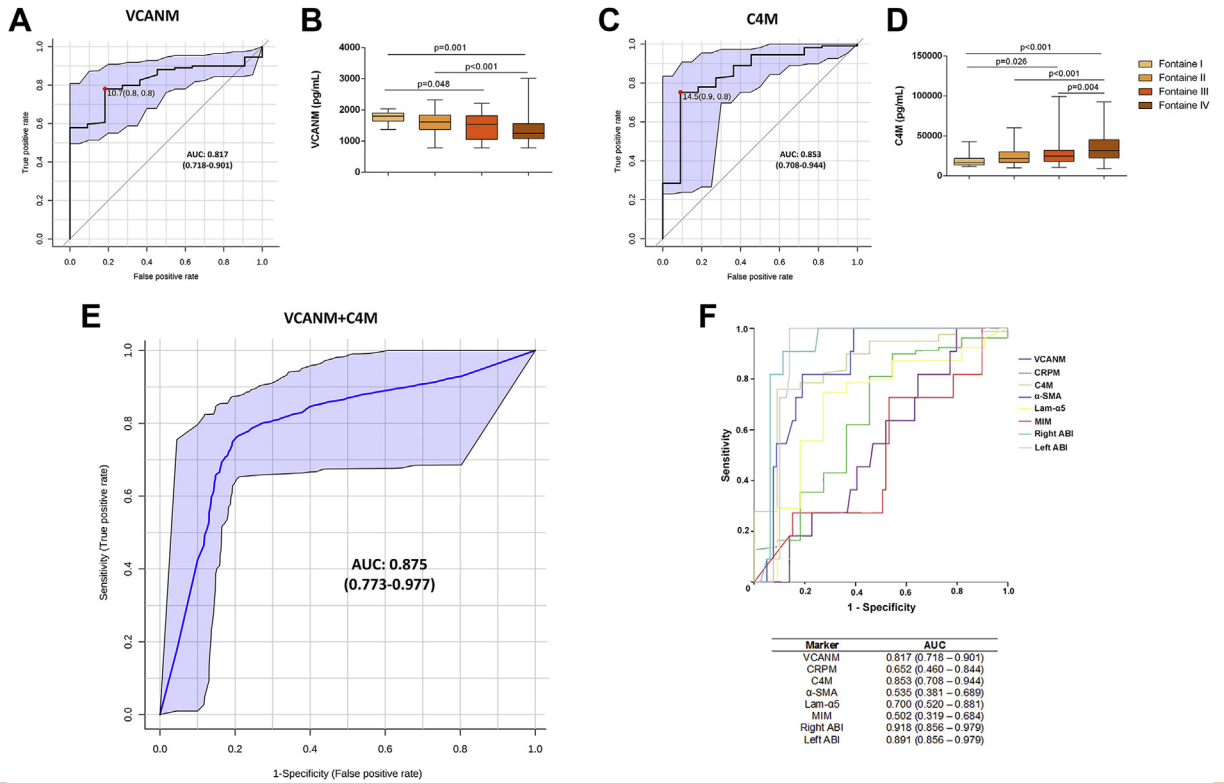

Fig 2. Candidate biomarkers. **A,** Receiver operating characteristic curve for VCANM measurements between Fontaine I and Fontaine IV patients. **B,** Graphical representation of VCANM concentrations among Fontaine grades. **C,** Receiver operating characteristic curve for C4M measurements between Fontaine I and Fontaine IV patients. **D,** Graphical representation of C4M concentrations among Fontaine grades. **E,** Receiver operating characteristic curve for the combination of VCANM and C4M obtained by binary logistic regression between Fontaine I and Fontaine IV patients. **F,** Receiver operating characteristic curve for all the candidate biomarkers compared with the ankle-brachial index (ABI), the standard technique to diagnose peripheral artery disease (PAD). *AUC,* Area under the curve.

tool for tracking atherosclerosis progression in the arterial wall tissue. Type IV collagen is a major component of basement membranes,[38] and these results are consistent with the observed alterations of the collagen network morphology apparently leading to deterioration of mechanical properties and propensity to rupture of the arterial wall. ABI showed the best discriminant capacity, but ECM markers provide complementary information to patients who are referred because of clinically suspected arterial disease, especially those with normal resting ABI.[39]

To our knowledge, this is the first study identifying neoepitope biomarkers of ECM remodeling as biomarkers for disease activity in LEAD. These measurements correlate with clinical end points and apparently provide clinically relevant information on processes reflecting atherosclerosis progression in lower extremity arteries. Exploring and re-evaluating the relationship between measurable biologic processes and clinical outcomes is crucial for deepening our knowledge on the role of arterial pathophysiologic changes in response to atherosclerosis. Whether these data reflect causality or document ECM changes during disease progression remains unknown.

The next level of evaluation needs other designs to ascertain predictive power in patients with asymptomatic PAD, and surrogate marker-defined efficacy calls for phase 4 follow-up studies. In this exploratory study, main limitations are the type of study and the common association of the disease with other cardiovascular disturbances. Future studies in prospective cohorts should consider the inclusion of women as well as the exclusion of coincident cardiovascular diseases and the usefulness of these markers after surgery. We envision that our proposed, laboratory-measured biomarkers may have the potential to speed drug development and to improve clinical awareness of the disease in primary care.

CONCLUSIONS

Severe lesions in PAD have a specific proteome compared with healthy arteries of age-matched controls. Our proteomics analysis indicates that inflammation and ECM turnover (ie, vascular remodeling) are the most quantitatively important processes in diseased arteries.

We propose versican and type IV collagen degradation products as potential laboratory-measured biomarkers of disease activity.

We acknowledge the technical assistance of the Centre for Omics Sciences and Servei de Recursos Científics i Tècnics (URV) in proteomics analysis and data interpretation.

AUTHOR CONTRIBUTIONS

Conception and design: VMP, JJ
Analysis and interpretation: AHA, SHN, CB, SFA, MF, MK, FG, JM, JC
Data collection: AHA, SHN, CB, SFA, VMP, MF
Writing the article: AHA, JJ
Critical revision of the article: AHA, SHN, CB, SFA, VMP, MF, MK, FG, JM, JC, JJ
Final approval of the article: AHA, SHN, CB, SFA, VMP, MF, MK, FG, JM, JC, JJ
Statistical analysis: AHA, SHN, CB, SFA, JC, JJ
Obtained funding: JM, JJ
Overall responsibility: JJ
AHA and SHN contributed equally to this article and share first authorship.

REFERENCES

1. Fowkes FG, Rudan D, Rudan I, Aboyans V, Denenberg JO, McDermott MM, et al. Comparison of global estimates of prevalence and risk factors for peripheral artery disease in 2000 and 2010: a systematic review and analysis. Lancet 2013;382:1329-40.
2. Camaré C, Pucelle M, Nègre-Salvayre A, Salvayre R. Angiogenesis in the atherosclerotic plaque. Redox Biol 2017;12:18-34.
3. Hazarika S, Annex BH. Biomarkers and genetics in peripheral artery disease. Clin Chem 2017;63:236-44.
4. Kim ES, Wattanakit K, Gornik HL. Using the ankle-brachial index to diagnose peripheral artery disease and assess cardiovascular risk. Cleveland Clin J Med 2012;79:651-61.
5. Chistiakov DA, Sobenin IA, Orekhov AN. Vascular extracellular matrix in atherosclerosis. Cardiol Rev 2013;21:270-88.
6. Xu J, Shi GP. Vascular wall extracellular matrix proteins and vascular diseases. Biochim Biophys Acta 2014;1842:2106-19.
7. Eble J, Niland S. The extracellular matrix of blood vessels. Curr Pharm Des 2009;15:1385-400.
8. Hansen NU, Genovese F, Leeming DJ, Karsdal MA. The importance of extracellular matrix for cell function and in vivo likeness. Exp Mol Pathol 2015;98:286-94.
9. Tanaka LY, Laurindo FR. Vascular remodeling: a redox-modulated mechanism of vessel caliber regulation. Free Radic Biol Med 2017;109:11-21.
10. Karsdal MA, Henriksen K, Leeming DJ, Woodworth T, Vassiliadis E, Bay-Jensen AC. Novel combinations of post-translational modification (PTM) neo-epitopes provide tissue-specific biochemical markers—are they the cause or the consequence of the disease? Clin Biochem 2010;43:793-804.
11. Genovese F, Karsdal MA. Protein degradation fragments as diagnostic and prognostic biomarkers of connective tissue diseases: understanding the extracellular matrix message and implication for current and future serological biomarkers. Expert Rev Proteomics 2016;13:213-25.
12. Rull A, Hernández-Aguilera A, Fibla M, Sepulveda J, Rodriguez-Gallego E, Riera-Borrull M, et al. Understanding the role of circulating chemokine (C-C motif) ligand 2 in patients with chronic ischemia threatening the lower extremities. Vasc Med 2014;19:442-51.
13. Hernández-Aguilera A, Sepulveda J, Rodriguez-Gallego E, Guirro M, Garcia-Heredia A, Cabre N, et al. Immunohistochemical analysis of paraoxonases and chemokines in arteries of patients with peripheral artery disease. Int J Mol Sci 2015;16:11323-38.
14. Vassiliadis E, Barascuk N, Karsdal MA. Atherofibrosis—a unique and common process of the disease pathogenesis of atherosclerosis and fibrosis—lessons for biomarker development. Am J Transl Med 2013;5:1-14.
15. Novo S. Classification, epidemiology, risk factors, and natural history of peripheral arterial disease. Diabetes Obes Metab 2002;4:S1-6.
16. Aragonès G, Auguet T, Guiu-Jurado E, Berlanga A, Curriu M, Martinez S, et al. Proteomic profile of unstable atheroma plaque: increased neutrophil defensin 1, clusterin, and apolipoprotein E levels in carotid secretome. J Proteome Res 2016;15:933-44.
17. Wiese S, Reidegeld KA, Meyer HE, Warscheid B. Protein labeling by iTRAQ: a new tool for quantitative mass spectrometry in proteome research. Proteomics 2007;7:340-50.
18. Rasmussen DG, Sand JM, Karsdal MA, Genovese F. Development of a novel enzyme-linked immunosorbent assay targeting a neo-epitope generated by cathepsin-mediated turnover of type III collagen and its application in chronic obstructive pulmonary disease. PLoS One 2017;12:e0170023.
19. Herwig R, Hardt C, Lienhard M, Kamburov A. Analyzing and interpreting genome data at the network level with ConsensusPathDB. Nat Protoc 2016;11:1889-907.
20. Huang CL, Wu IH, Wu YW, Hwang JJ, Wang SS, Chen WJ, et al. Association of lower extremity arterial calcification with amputation and mortality in patients with symptomatic peripheral artery disease. PLoS One 2014;9:e90201.
21. Abtan J, Bhatt DL, Elbez Y, Sorbets E, Eagle K, Reid CM, et al. Geographic variation and risk factors for systemic and limb ischemic events in patients with symptomatic peripheral artery disease: insights from the REACH Registry. Clin Cardiol 2017;40:710-8.
22. Bentzon JF, Otsuka F, Virmani R, Falk E. Mechanisms of plaque formation and rupture. Circ Res 2014;114:1852-66.
23. Li J, Liu X, Xiang Y, Ding X, Wang T, Liu Y, et al. Alpha-2-macroglobulin and heparin cofactor II and the vulnerability of carotid atherosclerotic plaques: an iTRAQ-based analysis. Biochem Biophys Res Commun 2017;483:964-71.
24. de Bruijne EL, Gils A, Rijken DC, de Maat MP, Guimaraes AH, Poldermans D, et al. High thrombin activatable fibrinolysis inhibitor levels are associated with an increased risk of premature peripheral arterial disease. Thromb Res 2011;127:254-8.
25. Ait-Oufella H, Kinugawa K, Zoll J, Simon T, Boddaert J, Heeneman S, et al. Lactadherin deficiency leads to apoptotic cell accumulation and accelerated atherosclerosis in mice. Circulation 2007;115:2168-77.
26. Wight TN, Merrilees MJ. Proteoglycans in atherosclerosis and restenosis: key roles for versican. Circ Res 2004;94:1158-67.
27. Gao Y, Wu W, Yu C, Zhong F, Li G, Kong W, et al. A disintegrin and metalloproteinase with thrombospondin motif 1 (ADAMTS1) expression increases in acute aortic dissection. Sci China Life Sci 2016;59:59-67.

28. Osorio FG, Navarro CL, Cadiñanos J, López-Mejía IC, Quirós PM, Bartoli C, et al. Splicing-directed therapy in a new mouse model of human accelerated aging. Sci Transl Med 2011;3:106ra107.
29. Zhang HJ, Wang J, Liu HF, Zhang XN, Zhan M, Chen FL, et al. Overexpression of mimecan in human aortic smooth muscle cells inhibits cell proliferation and enhances apoptosis and migration. Exp Ther Med 2015;10:187-92.
30. Karsdal MA, Nielsen MJ, Sand JM, Henriksen K, Genovese F, Bay-Jensen AC, et al. Extracellular matrix remodeling: the common denominator in connective tissue diseases. Possibilities for evaluation and current understanding of the matrix as more than a passive architecture, but a key player in tissue failure. Assay Drug Dev Technol 2013;11:70-92.
31. Genovese F, Barascuk N, Larsen L, Larsen MR, Nawrocki A, Li Y, et al. Biglycan fragmentation in pathologies associated with extracellular matrix remodeling by matrix metalloproteinases. Fibrogenesis Tissue Repair 2013;6:9.
32. Karsdal MA, Genovese F, Madsen EA, Manon-Jensen T, Schuppan D. Collagen and tissue turnover as a function of age: implications for fibrosis. J Hepatol 2016;64:103-9.
33. Sand JM, Larsen L, Hogaboam C, Martinez F, Han M, Røssel Larsen M, et al. MMP mediated degradation of type IV collagen alpha 1 and alpha 3 chains reflects basement membrane remodeling in experimental and clinical fibrosis—validation of two novel biomarker assays. PLoS One 2013;8:e84934.
34. Katsuda S, Kaji T. Atherosclerosis and extracellular matrix. J Atheroscler Thromb 2003;5:267-74.
35. Sand JM, Knox AJ, Lange P, Sun S, Kristensen JH, Leeming DJ, et al. Accelerated extracellular matrix turnover during exacerbations of COPD. Respir Res 2015;16:69.
36. Wight TN, Kang I, Merrilees MJ. Versican and the control of inflammation. Matrix Biol 2014;35:152-61.
37. Otsuka F, Kramer MC, Woudstra P, Yahagi K, Ladich E, Finn AV, et al. Natural progression of atherosclerosis from pathologic intimal thickening to late fibroatheroma in human coronary arteries: a pathology study. Atherosclerosis 2015;241:772-82.
38. Mao M, Alavi MV, Labelle-Dumais C, Gould DB. Type IV collagens and basement membrane diseases: cell biology and pathogenic mechanisms. Curr Top Membr 2015;76:61-116.
39. Stein R, Hriljac I, Halperin JL, Gustavson SM, Teodorescu V, Olin JW. Limitation of the resting ankle-brachial index in symptomatic patients with peripheral arterial disease. Vasc Med 2006;11:29-33.

Submitted Sep 24, 2017; accepted Dec 21, 2017.

Additional material for this article may be found online at www.jvascsurg.org.

INVITED COMMENTARY

Raul J. Guzman, MD, *Boston, Mass*

The search for relevant biomarkers that can track or predict peripheral artery disease (PAD) progression has recently accelerated because of the proliferation of new methods including proteomic and genetic analysis. In this manuscript, Dr Joven's group provides evidence for two novel serum biomarkers that can separate patients with mild and severe PAD. The peptides are degradation products of the matrix proteins versican and type IV collagen. To do this, they began by using histology and untargeted proteomics to identify a group of proteins in arterial specimens taken from PAD patients and normal controls. Using an unbiased approach, they demonstrated that 14 of the 81 initially identified proteins were differentially expressed between the two groups. Using these data, they next showed that serum levels of two of these peptides could be used to segregate patients with mild vs severe PAD symptoms.

Such an approach can be rewarding as it may yield new methods of identifying patients with PAD as well as those most likely to progress to more severe levels of disease. However, extensive clinical research will be required to determine the sensitivity and specificity of such markers and particularly whether these findings will hold up after adjusting for relevant demographic and cardiovascular risk factors. It is notable that there is a significant difference in diabetes prevalence between the two groups in this manuscript, and such factors will need to be included in future analyses. These data are nevertheless interesting, not only for the potential clinical applicability but also for the insights they provide into the basic pathophysiologic mechanisms that control peripheral atherosclerosis. The authors are to be commended for implementing such new (and laborious) techniques. No doubt that more biomarkers will be identified. Selection of the most valuable for clinical use will be our concern in the coming future.

The opinions or views expressed in this commentary are those of the authors and do not necessarily reflect the opinions or recommendations of the Journal of Vascular Surgery or the Society for Vascular Surgery.

SUPPLEMENTARY METHODS (online only).

Tissue collection, handling, and preservation

We have limited our study to samples obtained from superficial femoral arteries with occlusion or severe stenosis. This is because there are significant differences between femoral, superficial femoral, and tibial vessels in terms of size and pathophysiologic and morphologic features of the plaque. Portions of the artery included the entire artery wall. In diseased arteries, timing, handling, and preservation conditions were the same in all cases per protocol. Differences in timing were unavoidable for control arteries obtained in road accident victims. Age and anatomic area were especially considered. Handling and preservation of arterial specimens of deceased individuals and participants were kept to a minimum with immediate freezing and maintenance at −80°C until the analyses.

Proteomics protocol

Tissue processing and protein preparation. Stored frozen pieces of arteries were cut in 100-mg pieces and placed into tubes with 8 mg of type 1 collagenase in 2 mL of tris-$CaCl_2$ buffer. Samples were incubated at 37°C for 30 minutes with shaking. They were then centrifuged at 5000 rpm at 4°C, supernatants were stored at −80°C, and pellets were resuspended in 1.5 mL of urea lysis buffer +0.1% sodium dodecyl sulfate. Samples were homogenized using Precellys 24 (Bertin Technologies, Montigny-le-Bretonneux, France) at 5000 rpm for 10 seconds. Immediately, they were sonicated and then centrifuged again at 2100 rpm for 10 minutes at 4°C. Pellets were discarded, supernatants were transferred into new tubes and centrifuged at 14,000 rpm for 1 hour at 4°C, and proteins were precipitated with trichloroacetic acid. Samples were placed at 4°C for 24 hours and then centrifuged at 5000 rpm for 10 minutes at 4°C. Supernatants were rejected and pellets resuspended in 1 mL of cold acetone. Samples were again centrifuged at 5000 rpm for 10 minutes at 4°C, supernatants were rejected, and pellets were resuspended in 0.5 M triethylammonium bicarbonate (TEAB) at pH 8.5. Protein quantification was performed, and samples were stored at −80°C.

Protein digestion and validation. After being vacuum dried, samples were resuspended in 0.5 M TEAB at pH 7, and 2% sodium dodecyl sulfate was added to denature proteins. Samples were reduced using 5 mM tris(2-carboxyethyl)phosphine in 50 mM TEAB at pH 7.9 for 1 hour at 60°C and then alkylated with 3.65 mM iodoacetamide during 30 minutes at room temperature in the dark. For the digestion, samples were incubated with 1 μg/μL sequencing-grade trypsin in 500 mM TEAB at pH 7.9 overnight at 37°C. Digestions were checked by analyzing a small aliquot using matrix-assisted laser desorption ionization time-of-flight mass spectrometry (MS) or nano-liquid chromatography. Peptides were separated onto a C18 reversed phase nanocolumn (75-μm inner diameter [ID], 15-cm length, 3-μm particle diameter; Nikkyo Technos Co LTD, Tokyo, Japan) coupled with a trap nano-column (100-μm ID, 2-cm length, 5-μm particle diameter; Thermo Fisher Scientific, San Jose, Calif). Digested samples were analyzed by injecting an 18-μL sample, using a continuous acetonitrile gradient of 0% to 35% in 13 minutes, 35% to 80% in 7 minutes, and 80% to 100% in 5 minutes. In all the analysis, a flow rate of 300 nL/min was used to elute peptides for real-time ionization and peptide fragmentation on an LTQ Orbitrap Velos Pro mass spectrometer (Thermo Fisher). An enhanced Fourier transform (FT)-resolution spectrum (resolution = 30,000 full half-maximum width [FHMW]) followed by data-dependent tandem MS (MS/MS) scan (R = 15,000 FHMW) from most intense 10 parent ions with a charge state rejection of 1 was analyzed along the chromatographic run. The MS/MS scan was acquired in the FT analyzer using a higher energy collision dissociation collision cell with a normalized collision energy of 45 and dynamic exclusion of 0.5 minute.

Isobaric tag for relative and absolute quantitation (iTRAQ) labeling. iTRAQ 8-plex labeling reagents (SCIEX, Madrid, Spain) were added to samples according to the manufacturer's instructions and incubated at room temperature for 2 hours. Quantification results are expressed as ratios of the different labeling tags vs a control tag, and these ratios were used for statistical purposes.

Labeled samples were purified using an SCX column (Strata SCX 55 μm, 70Å; Phenomenex, Torrance, Calif). Then, they were desalted and concentrated through a C18 Sep-Pak column (Waters, Bedford, Mass). Eluted peptides were dried and resuspended in 0.1% (v/v) formic acid for nano-liquid chromatography-MS/MS detection. Labeled iTRAQ peptides were separated onto a C18 reversed phase nanocolumn (75-μm ID, 15-cm length, 3-μm particle diameter; Nikkyo Technos Co LTD) coupled to a trap nanocolumn (100-μm ID, 2-cm length, 5-μm particle diameter; Thermo Fisher Scientific). All samples were analyzed in triplicate. For each analysis, 2 μg of sample was injected using a continuous acetonitrile gradient consisting of 0% to 5% B in 4 minutes, 5% to 15% B in 60 minutes, 15% to 35% B in 60 minutes, and 35% to 95% B in 10 minutes, which was maintained for 20 minutes (A = water, 0.1% formic acid; B = acetonitrile, 0.1% formic acid). In all the analysis, a flow rate of 300 nL/min was used to elute peptides for real-time ionization and peptide fragmentation on an LTQ ObritrapVelo sPro mass spectrometer (Thermo Fisher). An enhanced FT-resolution spectrum (resolution = 30,000 FHMW) followed by data-dependent MS/MS scan (R = 15,000 FHMW) from most intense parent ions was analyzed throughout the chromatographic run. The MS/MS scan

was acquired in the FT analyzer using a higher energy collision dissociation collision cell with normalized collision energy of 45%, a precursor mass window selection of 2 m/z, a charge state rejection of +1, and a dynamic exclusion of 0.5 minute.

Protein identification analysis. Tandem mass spectra were extracted and charge state deconvoluted by Proteome Discoverer version 1.4.0.288 (Thermo Fisher Scientific). All MS and MS/MS samples were analyzed using Mascot (version 2.4.1.0; Thermo Fisher Scientific). Mascot was set up to search SwissProt_2012_03.fasta database (535248 entries), restricting for human taxonomy (26944 sequences) and assuming trypsin digestion. Two missed cleavages were allowed, and an error of 0.02 Da for fragment ion mass and 10.0 ppm for a parent ion were allowed. Oxidation of methionine, acetylation of N-termini, and iTRAQ 8-plex were specified as variable modifications, whereas carbamidomethylation of cysteine was set as static modification. The false discovery rate and protein probabilities were calculated by Target Decoy PSM Validator working between 0.01 and 0.05 for strict and relaxed, respectively. For proteins identified with only one peptide, visual verification of fragmentation spectra was done.

Quantitative proteome analysis. In tandem MS mode, which isolates and fragments peptides, each tag generates a unique reporter ion used for a relative quantification. Protein quantification compares the peak intensity of the reporter ions in the MS/MS spectra to assess the relative abundance of the peptides and the proteins from which they are derived. The quantification method allows normalization with filters to measure the abundance of proteins in the sample using unique peptides of each protein.

Enzyme-linked immunosorbent assay protocol. The enzyme-linked immunosorbent assays were technically validated according to the Nordic Bioscience standard operating procedures. Linearity, lower limit of detection, intravariation and intervariation, spiking recovery, and assay stability were assessed. Protocols and buffers differ among assays. In general, a 96-well streptavidin precoated plate was coated with the selected biotinylated synthetic peptide dissolved in specific buffer and incubated. The peptide calibrator or sample was added to appropriate wells, followed by the horseradish peroxidase-conjugated monoclonal antibody, and again incubated. Finally, 3,3′,5,5′-tetramethylbenzidine developer (cat.438OH; Kem-En-Tec, Taastrup, Denmark) was added, and the plate was incubated in the dark. All these incubation steps included shaking. After each incubation step, the plates were washed in washing buffer. The reaction was stopped by adding stopping solution (0.1 M H_2SO_4) and measured at 450 to 650 nm. A standard calibration curve was also plotted.

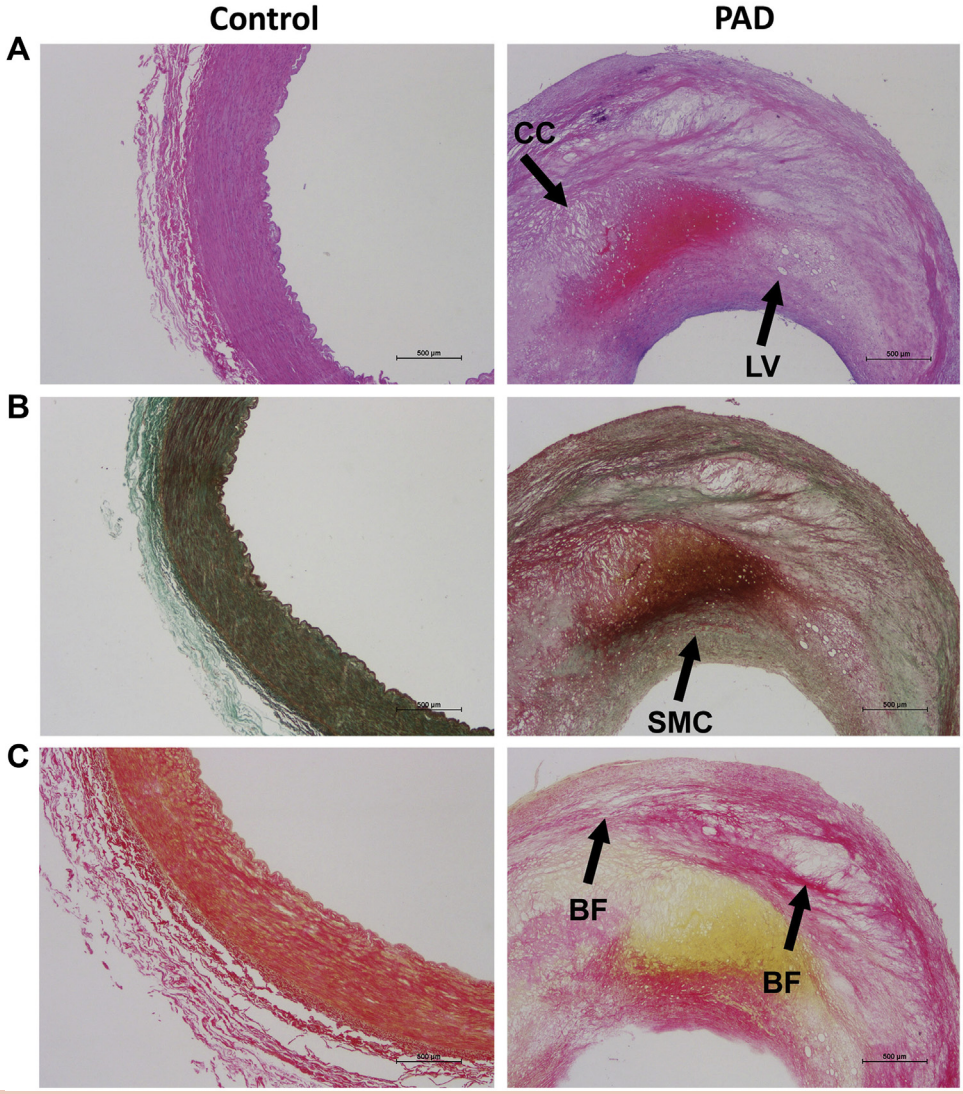

Supplementary Fig (online only). Representative histologic findings in peripheral arteries from control group and peripheral artery disease (*PAD*) patients (magnification ×200). Hematoxylin and eosin **(A),** Masson trichrome **(B),** and sirius red **(C)** stains were used for assessment. The tunica intima was disorganized and thicker, and the presence of lipid vacuoles and cholesterol crystals and other histologic features were consistent with the higher ($P < .0001$) intima-media ratio observed in PAD patients (median, 2.10 [interquartile range, 1.33-3.22]) with respect to that of age-matched donors (median, 0.16 [interquartile range, 0.13-0.65]). Smooth muscle cells, normally located in the media, were also present in the intima of atherosclerotic arteries. The distribution of collagen fibers was also disrupted. *BF,* Broken fibers of collagen; *CC,* cholesterol crystals; *LV,* lipid vacuoles; *SMC,* smooth muscle cells.

Supplementary Table I (online only). Clinical characteristics, complete blood count, and biochemical characteristics of control individuals and peripheral artery disease (*PAD*) patients

	Controls (n = 3)	PAD patients (n = 18)	*P* value
Clinical characteristics			
Age, years	75 (0.707)	69 (12)	NS
BMI, kg/m^2	26.7 (2.3)	26.3 (6.0)	NS
Diabetes	1	13	.05
Hypertension	1	9	NS
Dyslipidemia	1	9	NS
Complete blood count			
Red blood cells, $\times10^{12}$/L	4.46 (0.21)	3.36 (0.33)	NS
Hemoglobin, g/dL	13.3 (1.2)	10.6 (0.7)	NS
Leukocytes, $\times10^9$/L	8.6 (0.9)	9.6 (4.7)	NS
Platelets, $\times10^9$/L	246 (27)	204 (12)	NS
Biochemical variables			
Total cholesterol, mmol/L	6.01 (1.72)	5.2 (0.28)	NS
Triglycerides, mmol/L	1.62 (1.14)	0.86 (0.31)	NS
Glucose, mmol/L	6.16 (0.92)	7.9 (2.2)	NS
Fibrinogen, g/L	5.92 (1.53)	5.80 (1.95)	NS

BMI, Body mass index; *NS,* not significant.
Nonparametric variables are shown as mean (standard deviation). Qualitative variables are expressed as number of total participants. Statistical differences were assessed by Mann-Whitney *U* test.

Supplementary Table II (online only). Overview of measured biomarkers to assess extracellular matrix (ECM) degradation in serum

Biomarker	Measurement	Reference	Upper normal level in general population, pg/mL
VCANM	Specific fragment of MMP-8- and MMP-12-mediated degradation of versican	1	1500
CRPM	Specific fragment of MMPs 1-, 3-, 8-, and 9-, CatS/K-, ADAMTS-mediated degradation of C-reactive protein	2	7500
C4M	Specific fragment of MMP-12-mediated type IV collagen (α1)	3	21,500
Lam-a5	Specific fragment of MMP-9 mediated laminin (α5)	Unpublished	10,166
α-SMA	Acetylated N-terminal fragment of α-smooth muscle actin	4	1480
MIM	Specific fragment of MMP-9- and MMP-12-mediated degradation of mimecan	5	5050

MMP, Matrix metalloproteinase.
1. Barascuk N, Genovese F, Larsen L, Byrjalsen I, Zheng Q, Sun S, et al. A MMP derived versican neo-epitope is elevated in plasma from patients with atherosclerotic heart disease. Int J Clin Exp Med 2013;6:174–184.
2. Skjøt-Arkil H, Schett G, Zhang C, Larsen DV, Wang Y, Zheng Q, et al. Investigation of two novel biochemical markers of inflammation, matrix metalloproteinase and cathepsin generated fragments of C-reactive protein, in patients with ankylosing spondylitis. Clin Exp Rheumatol 2012;30:371–379.
3. Sand JM, Larsen L, Hogaboam C, Martinez F, Han M, Røssel Larsen M, et al. MMP mediated degradation of type IV collagen alpha 1 and alpha 3 chains reflects basement membrane remodeling in experimental and clinical fibrosis—validation of two novel biomarker assays. PLoS One 2013;8:e84934.
4. Papasotiriou M, Genovese F, Klinkhammer BM, Kunter U, Nielsen SH, Karsdal MA, et al. Serum and urine markers of collagen degradation reflect renal fibrosis in experimental kidney diseases. Nephrol Dial Transplant 2015;30:1112–1121.
5. Barascuk N, Vassiliadis E, Zheng Q, Wang Y, Wang W, Larsen L, et al. Levels of circulating MMCN-151, a degradation product of mimecan, reflect pathological extracellular matrix remodeling in apolipoprotein E knockout mice. Biomark Insights 2011;6:97–106.

Supplementary Table III (online only). Proteins identified in human healthy control arteries and peripheral artery disease (PAD) arteries by untargeted proteomics (in alphabetical order)

Swiss-prot ID	Compound name	Biologic function
P60709	Actin, cytoplasmic 1	ATP binding
P63267	Actin, γ-enteric smooth muscle	ATP binding
P01009	α_1-Antitrypsin	Glycoprotein, protease and binding
P01023	α_2-Macroglobulin	Enzyme, growth factor and protease binding
O43707	α-Actinin 4	Involved in vesicular trafficking through its association with the CART complex
P04114	Apolipoprotein B-100	Cholesterol transporter activity
P02649	Apolipoprotein E	Mediates the binding, internalization, and catabolism of lipoprotein particles
P25705	ATP synthase subunit α, mitochondrial	Transmembrane transporter activity
P02730	Band 3 anion transport protein	Transporter mediates electroneutral anion exchange across the cell membrane
P98160	Basement membrane-specific heparan sulfate proteoglycan core protein	Metal ion and protein C-terminus binding
P51911	Calponin 1	Regulation of smooth muscle contraction
P00915	Carbonic anhydrase 1	Arylesterase activity
Q96IY4	Carboxypeptidase B2	Metallocarboxypeptidase activity
P07339	Cathepsin D	Aspartic-type endopeptidase activity
P00450	Ceruloplasmin	Chaperone and copper ion binding
P10909	Clusterin	Chaperone, misfolded protein, and ubiquitin protein ligase binding
P00488	Coagulation factor XIII A chain	Metal ion binding
P12109	Collagen α1(VI) chain	Platelet-derived growth factor binding
Q99715	Collagen α1(XII) chain	Extracellular matrix structural constituent conferring tensile strength
Q05707	Collagen α1(XIV) chain	Extracellular matrix structural constituent
P08123	Collagen α2(I) chain	Extracellular matrix structural constituent
P12110	Collagen α2(VI) chain	Collagen VI acts as a cell-binding protein
P12111	Collagen α3(VI) chain	Serine-type endopeptidase inhibitor activity
P01024	Complement C3	C5L2 anaphylatoxin chemotactic receptor, cofactor, endopeptidase inhibitor, and lipid binding
P07360	Complement component C8 γ chain	Retinol binding
P02748	Complement component C9	Constituent of the membrane attack complex
P00403	Cytochrome *c* oxidase subunit 2	Cytochrome *c* oxidase activity
P60981	Destrin	Actin polymerization or depolymerization
P35555	Fibrillin 1	Extracellular matrix constituent conferring elasticity
P02671	Fibrinogen α chain	Metal ion binding
P02675	Fibrinogen β chain	Chaperone binding
P02679	Fibrinogen γ chain	Cell adhesion molecule binding
P02751	Fibronectin	Heparin, integrin, mercury ion, protease, and collagen binding
Q9UBX5	Fibulin 5	Calcium, integrin, protein C-terminus binding
P21333	Filamin A	Promotes orthogonal branching of actin filaments and links actin filaments to membrane glycoproteins
P06396	Gelsolin	Actin, calcium, myosin II, and protein domain specific binding
P04406	Glyceraldehyde-3-phosphate dehydrogenase	Microtubule binding
P00738	Haptoglobin	Hemoglobin binding
P69905	Hemoglobin subunit α	Oxygen transporter activity
P68871	Hemoglobin subunit βa	Oxygen transporter activity

(Continued on next page)

Supplementary Table III (online only). Continued.

Swiss-prot ID	Compound name	Biologic function
P02790	Hemopexin	Metal ion binding
O60814	Histone H2B type 1-K	DNA binding
P01876	Ig α1 chain C region	Antigen binding
P01857	Ig γ1 chain C region	Antigen binding
P01859	Ig γ2 chain C region	Antigen binding
P01765	Ig heavy chain V-III region TIL	Antigen binding
P01834	Ig κ chain C region	Antigen binding
P01617	Ig κ chain V-II region TEW	Antigen binding
P01619	Ig κ chain V-III region B6	Antigen binding
P04433	Ig κ chain V-III region VG (fragment)	Antigen binding
P01717	Ig λ chain V-IV region Hil	Antigen binding
P0CG04	Ig λ1 chain C regions	Antigen binding
A0M8Q6	Ig λ7 chain C region	Antigen binding
P01871	Ig μ chain C region	Antigen binding
Q14624	Inter-α-trypsin inhibitor heavy chain H4	Serine-type endopeptidase inhibitor and endopeptidase inhibitor activity
Q08431	Lactadherin	Phosphatidylethanolamine and phosphatidylserine binding
O15230	Laminin subunit α5	Integrin binding
P11047	Laminin subunit γ1	Extracellular matrix structural constituent
Q16853	Membrane primary amine oxidase	Cell adhesion protein
P35580	Myosin 10	Actin filament binding
P35749	Myosin 11	DNA binding
P59665	Neutrophil defensin 1	Has antimicrobial activity against gram-negative and gram-positive bacteria
Q15063	Periostin	Metal, cell adhesion molecule, and heparin binding
P32119	Peroxiredoxin 2	Antioxidant and thioredoxin peroxidase activity
P00747	Plasminogen	Apolipoprotein binding
P02545	Prelamin A/C	Structural molecule activity
Q9NQH7	Probable Xaa-Pro aminopeptidase 3	Aminopeptidase and metallopeptidase activity
P02760	Protein AMBP	Inhibits calcium oxalate crystallization
P14618	Pyruvate kinase isozymes M1/M2	Glycolytic enzyme
Q13228	Selenium-binding protein 1	Selenium binding
P02787	Serotransferrin	Transport of iron from sites of absorption and heme degradation to those of storage and utilization
P02743	Serum amyloid P-component	Calcium ion, virion, unfolded protein, and carbohydrate binding
P24821	Tenascin	Syndecan binding
P07996	Thrombospondin 1	Adhesive glycoprotein that mediates cell-to-cell and cell-to-matrix interactions
P29401	Transketolase	Cofactor and metal binding
P68366	Tubulin α4A chain	Structural constituent of cytoskeleton
O00159	Unconventional myosin Ic	ATP binding
P13611	Versican core protein	Calcium, carbohydrate, glycosaminoglycan, and hyaluronic acid binding
P08670	Vimentin	Vimentin is attached to the nucleus, endoplasmic reticulum, and mitochondria
P04004	Vitronectin	Vitronectin interacts with glycosaminoglycans and proteoglycans
O75083	WD repeat-containing protein 1	Induces disassembly of actin filaments in conjunction with ADF/cofilin family proteins

ADF, Actin-depolymerizing factor; *ATP,* adenosine triphosphate; *CART,* cytoskeleton-associated recycling or transport; *Ig,* immunoglobulin.